

## Crystal Structure of ZnTe III at 16 GPa

R. J. Nelmes, M. I. McMahon, N. G. Wright, and D. R. Allan  
*Department of Physics and Astronomy, The University of Edinburgh,  
Mayfield Road, Edinburgh, EH9 3JZ, United Kingdom*  
(Received 16 May 1994)

The long-uncertain crystal structure of ZnTe phase III, stable above 11 GPa, has been determined at 16 GPa using angle-dispersive powder-diffraction techniques with an image-plate area-detector and synchrotron radiation. The structure is orthorhombic, space group *Cmcm*, and is site ordered. This is a new high-pressure structure, which can be derived by distortion of the rocksalt structure. But the coordination is quite different from NaCl: There are only five nearest neighbors (all unlike) around each atom at  $\sim 2.7$  Å and then three next-nearest-neighbors (of which two are like atoms) at 3.0–3.4 Å.

PACS numbers: 61.50.Ks, 62.50.+p

Studies of the II-VI semiconductor ZnTe have long been impeded by uncertainties as to the structures of its high-pressure phases. All the evidence has been that it exhibits more complex structural behavior than the other zinc chalcogenides ZnS and ZnSe, which transform from zinc blende directly to NaCl [1,2], and the other tellurides CdTe and HgTe, which transform from zinc blende first to the cinnabar structure and then to NaCl [3,4]. Interest in the high-pressure phases of ZnTe was first aroused by the resistivity measurements of Samara and Drickamer [5], which revealed three sharp discontinuities in the conductivity of ZnTe below 15 GPa. Subsequent diffraction measurements [1] showed that two of these discontinuities correspond to structural phase transitions. Further resistivity measurements [6] suggested transition pressures of 8.5 GPa (to nonmetallic ZnTe II) and 13 GPa (to metallic ZnTe III), but the quality of data from complementary x-ray diffraction studies was insufficient to determine the structure of either of the high-pressure phases. More recent diffraction and optical studies [7] gave revised values for the transition pressures of 9.3 and 11.0 GPa and some partial structural information. Although it was still not possible to determine the structure of ZnTe II, the diffraction data did allow both the NaCl and  $\beta$ -tin structures to be excluded. The diffraction pattern for ZnTe III, which was found to be stable to at least 30 GPa, contained 10 observable peaks which could be indexed on a monoclinic unit cell. However, no specific structure was reported.

A combined extended x-ray absorption fine structure (EXAFS) and (energy-dispersive) x-ray diffraction study [8] has recently proposed the cinnabar structure for ZnTe II, which suggests that ZnTe does in fact follow the same transition sequence as CdTe and HgTe initially. The results obtained for ZnTe III indicate that a minimum pressure of 14–15 GPa is needed to establish an entirely single phase, but the structure still remains unclear. No simple coordination model gave a good fit to the EXAFS data; the best was achieved with sixfold, NaCl-like coordination and a large value of the pseudo-Debye-Waller factor, possibly compatible with the monoclinic

symmetry found in earlier diffraction work. The actual structure of ZnTe III, and the difference between this phase and those known for all the other II-VI systems, thus still remained as a significant unsolved problem.

As part of a systematic study of the II-V, II-VI, and group IV semiconductors at high pressure, we have now determined the crystal structure of ZnTe III using angle-dispersive diffraction techniques, coupled with an image-plate area detector and synchrotron radiation. We also confirm the cinnabar structure (possibly with a small distortion) for the ZnTe-II phase. We find that ZnTe III has a site-ordered orthorhombic structure with space group *Cmcm* and unusual, fivefold coordination which can be understood as a strong distortion of the NaCl structure. This structure has not previously been reported for any high-pressure phase. However, preliminary results on other II-VI systems [9] suggest that this structure may be common to them, too, and thus play an important role in the overall structural systematics.

Diffraction data were collected at room temperature on station 9.1 at the synchrotron radiation source, Daresbury, using angle-dispersive diffraction techniques and an image-plate area detector. All experiments were carried out with a calibrated wavelength of 0.4648(1) Å, except for studies of anomalous dispersion effects near the Te *K* edge. Details of our experimental setup and pattern integration program have been reported previously [10–12]. Full conical aperture Diacell DXR-4 [13] and Merrill-Bassett diamond-anvil pressure cells were used, with diamond culet diameters of 600  $\mu\text{m}$ . The sample was a finely ground powder prepared from a single-crystal sample, from the same source as Ref. [8]. Samples were loaded with a 4:1 mixture of methanol:ethanol as the pressure-transmitting medium, and the pressure was measured using the ruby-fluorescence technique [14]. All structural parameters, including lattice parameters, were obtained from Rietveld refinement [15] of the full integrated profiles using the program MPROF [16].

On pressure increase the well known transition from the zinc blende phase to ZnTe II was observed just below 9 GPa. A single-phase pattern of ZnTe II collected at

8.9 GPa is shown in Fig. 1(a). When the sample pressure was increased above 11 GPa, we obtained a mixed-phase sample of ZnTe II and ZnTe III. A mixed-phase pattern collected at 11.5 GPa is shown in Fig. 1(b). A further increase in pressure to 15.7 GPa—above the range of possible residual phase mixing [8]—gave high-quality single-phase patterns of ZnTe III, as illustrated in Fig. 1(c). A good fit to the ZnTe II pattern in Fig. 1(a) was obtained with the cinnabar structure and refined lattice parameters of  $a = 4.105(1)$  and  $c = 9.397(1)$  Å [17]. Small but significant differences between the observed and calculated positions of two reflections indicate a possible slight distortion from the ideal cinnabar structure. This and the details of the structure will be published separately [17].

In the ZnTe-III pattern of Fig. 1(c) it was possible to measure the positions of 15 reflections, including the very weak reflection at  $6.6^\circ$  shown in the inset. Using the indexing program DICVOL, an excellent fit to the data was found to be given by an orthorhombic unit cell with lattice parameters of  $a = 5.38$ ,  $b = 5.97$ , and  $c = 5.01$  Å. The pattern could then be indexed, and this revealed reflections with  $h + k = \text{odd}$  in all  $(hkl)$  and  $l = \text{odd}$  in  $(h0l)$  to be systematically absent. The lattice symmetry is thus  $C$ -face centered. For a physically reasonable density, the unit cell must have a four-atom basis.

The reflection in the inset of Fig. 1 indexes as  $(110)$ . The inset shows, on a common intensity scale, this reflection collected at incident wavelengths far ( $f$ ) from and near ( $n$ ) to the Te  $K$  edge. [The shift in  $2\theta$  results from this wavelength change.] The clear change in intensity

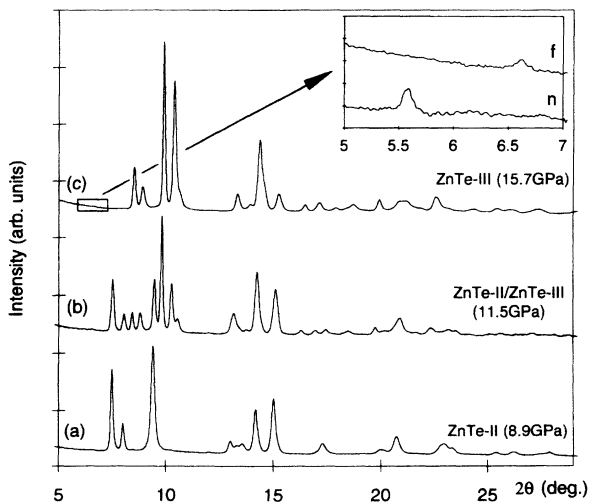


FIG. 1. Integrated profiles of the patterns recorded from ZnTe on pressure increase. (a) A single-phase ZnTe-II profile collected at 8.9 GPa, (b) a mixed-phase ZnTe-II/ZnTe-III profile collected at 11.5 GPa, and (c) a single-phase ZnTe-III profile collected at 15.7 GPa. The inset shows an enlarged view of the weak  $(110)$  reflection in profile (c), recorded at 27.925 keV, far ( $f$ ) from the Te  $K$  edge, and at 31.747 keV, near ( $n$ ) the Te  $K$  edge (at 31.813 keV).

1806

shows the ZnTe-III structure to be site ordered [18]. The systematic absence conditions given above restrict possible space groups to  $Cmcm$ ,  $C2cm$ , and  $Cmc2_1$ . It is worth noting that only the very weak  $(110)$  reflection rules out two other space groups,  $C2cb$  and  $Cmca$ —all other reflections with  $h$  and  $k$  both odd are overlapped. The three possible groups all have eightfold or 16-fold general positions. But the site ordering restricts possible structures to fourfold special positions. Those consistent with the observed absences are  $4(c)$  of  $Cmcm$ ,  $4(b)$  of  $C2cm$ , and  $4(a)$  of  $Cmc2_1$ . [The absences are also consistent with the  $4(b)$  special position of  $C222_1$ , but this is not distinguishable from  $4(c)$  of  $Cmcm$  and therefore need not be considered further—by convention, the higher symmetry group is adopted in such circumstances.]

The 2D images collected from ZnTe III showed evidence of strong preferred orientation in the sample, and this was investigated further before attempting full structure analysis. Images recorded with the axis of the pressure cell inclined to the incident beam revealed that the  $(002)$  reflection is strongly affected. This is shown in the inset to Fig. 2, where the observed intensity of  $(002)$  can be seen to be increased significantly at an inclination of  $30^\circ$ —the maximum useful angle with present experimental facilities. Calculations show that the apparent suppression of a reflection by preferred orientation is relatively little altered by an inclination of  $30^\circ$ , so the true intensity is considerably greater than it is in the profile of Fig. 1(c). But the preferred orientation effects on the other main reflections, labeled in Fig. 2, were found to be relatively small (see the inset). The observed intensities of the  $(200)$ ,  $(021)$ , and  $(020)$  reflections can then be used to obtain the approximate structure. The relative strength of  $(200)$ , despite its low multiplicity, indicates that the atoms are all on, or close to,  $(200)$  planes; the strength of  $(021)$ , and the relative weakness of  $(020)$ , shows that all atoms must also be close to  $(002)$  and sepa-

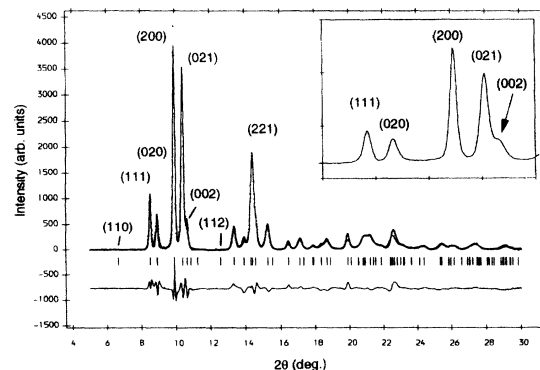


FIG. 2. Fit to the single-phase ZnTe-III in Fig. 1(c). The tick marks show the positions of all the reflections allowed by symmetry. The difference between the observed and calculated profiles is displayed below the tick marks. The inset shows the low-angle part of the profile collected with the axis of the pressure cell inclined at  $30^\circ$  to the incident beam.

rated by  $\sim 1/4$  in  $y$ . [This would give a strong (002) reflection, in accord with the observed preferred orientation effects.] The required arrangement corresponds to the 4(c) position of  $Cmcm$  ( $0, y, 1/4; 0, -y, 3/4; 1/2, 1/2 + y, 1/4; 1/2, 1/2 - y, 3/4$ ) with one atom at  $y \sim 1/8$  and the other at  $y \sim 5/8$ . This is an orthorhombically distorted NaCl structure, with alternate (001) planes displaced  $\pm 1/8$  along the  $b$  axis. Special positions 4(b) of  $C2cm$  and 4(a) of  $Cmc2_1$  allow additional relative displacements along  $x$  and  $z$ , respectively, but the strength of the (200) and (021) reflections indicates that any such displacements are small. Therefore refinements were first carried out in  $Cmcm$ , starting from the above coordinates and (arbitrarily) selecting Te to be at  $y \sim 1/8$ .

The variables in the structure refinement were a scale factor, the  $a$ ,  $b$ , and  $c$  lattice parameters, the two variable atomic coordinates  $y(\text{Zn})$  and  $y(\text{Te})$ , two isotropic thermal-motion parameters, three peak-shape parameters, and a preferred orientation parameter. The crystallographic axis of the preferred orientation was chosen to reduce the (002) reflection intensity strongly and then iteratively fine-tuned to optimize the fit to the other affected reflections. The resulting best fit is shown in Fig. 2. Trial refinements were also carried out in  $C2cm$  and  $Cmc2_1$ , and these gave small additional displacements of  $\sim 0.02$  in  $x$  and  $\sim 0.05$  in  $z$ , respectively. However, even these small displacements result in calculated intensities stronger than observed for the very weak (110) and (112) reflections, and it was concluded that there is no evidence for symmetry lower than  $Cmcm$ .

The best fit shown in Fig. 2 was obtained with refined lattice parameters  $a = 5.379(1)$ ,  $b = 5.971(1)$ , and  $c = 5.010(2)$  Å, and atomic coordinates  $y(\text{Te}) = 0.190(1)$  and  $y(\text{Zn}) = 0.640(1)$ . The separation in  $y$  coordinates is thus quite different from 0.5. This was tested by carrying out refinements with  $y(\text{Zn}) - y(\text{Te})$  constrained to 0.5. The results showed that this arrangement cannot give the observed weak (110) intensity without making the (020) intensity much greater than observed—and other significant misfits. In the best-fitting structure, the nearest-neighbor (in the same  $yz$  plane) to the Te atom at  $(0, 0.190, 1/4)$  is the Zn atom at  $(0, 0.360, 3/4)$ —see Fig. 3. Another possible solution to the structure has to be considered in which these nearest neighbors are like atoms. This distinct structure—with quite different coordination—was found to give a stable refinement and a fit that was evidently poorer but not clearly unacceptable apart from the (110) reflection. This was calculated much stronger than observed; and if atomic coordinates were constrained to give a weak (110) intensity, then larger discrepancies were obtained for other reflections. This alternative is thus excluded in favor of the structure shown in Fig. 3, which is also more plausible in having unlike atoms as nearest neighbors. The few remaining small misfits discernible in Fig. 2 are almost certainly attributable to the inability of a simple, one-parameter model to account completely for the (pronounced) preferred orientation.

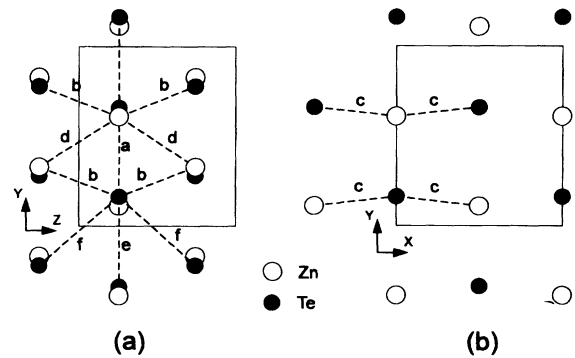


FIG. 3. The  $Cmcm$  structure of ZnTe-III viewed along the  $x$  and  $z$  axes. The dashed lines mark the nearest-neighbor contacts around the Zn atom at  $(0, 0.640, 1/4)$  and the Te atom at  $(0, 0.190, 1/4)$ . The letters label the six different nearest- and next-nearest-neighbor distances.

The final structure was then used as a starting point for a two-phase refinement of the ZnTe-II/ZnTe-III pattern shown in Fig. 1(b), assuming the ideal cinnabar structure for ZnTe II, as refined for the Fig. 1(a) profile. The best-fitting lattice parameters for the two phases at 11.5 GPa are  $a = 4.085(1)$  and  $c = 9.315(4)$  Å for ZnTe II, and  $a = 5.436(1)$ ,  $b = 6.050(1)$ , and  $c = 5.058(2)$  Å for ZnTe III. The change in specific volume at the transition is thus  $\Delta V/V_0 = 5.7(2)\%$ , where  $V_0$  is  $21.409(5)$  Å<sup>3</sup> from the refined lattice parameter of the zinc blende phase at ambient pressure.

Figure 3(a) shows the structure projected down the  $x$  axis, with the atoms at  $x = 0$  overlapping those at  $x = 1/2$ . The dashed lines mark nearest-neighbor contacts around the Zn atom at  $(0, 0.640, 1/4)$  and the Te atom at  $(0, 0.190, 1/4)$ . Figure 3(b) shows the single  $xy$  plane at  $z = 1/4$  and the nearest-neighbor contacts along the  $x$  direction. And the letters label the six different nearest- and next-nearest-neighbor distances, which are 2.687(8), 2.703(3), 2.706(1), 3.012(5), 3.284(8), and 3.380(6) Å in the sequence “a” to “f”.

The structure can be considered as a distortion of the NaCl structure. From Fig. 3(b) it can be seen that the atoms are all in flat NaCl-like planes perpendicular to  $z$ , but distorted from true NaCl by (i) the difference between the  $a$  and  $b$  lattice parameters and (ii) the zigzag arising from  $y(\text{Zn}) - y(\text{Te}) \neq 0.5$ . Alternate NaCl-like planes are displaced approximately  $+0.08$  and  $-0.08$  along  $y$ , which produces a marked zigzag along  $z$  [Fig. 3(a)] and a 3D coordination quite different from NaCl. In fact the coordination is very approximately simple hexagonal, with eight contacts around each atom. However, these differ considerably in length, and the close coordination is only fivefold. Both Zn and Te have five (unlike) nearest neighbors at  $\sim 2.7$  Å, compared with four at  $\sim 2.6$  Å in the cinnabar phase at 8.9 GPa [18]. The next-nearest unlike neighbor for the Zn atom is at  $\sim 3.3$  Å, farther away than the two Zn-Zn contacts at  $\sim 3.0$  Å. The Te atom also has its next-nearest unlike neighbor at  $\sim 3.3$  Å,

but the nearest Te-Te contacts are at  $\sim 3.4$  Å. And the close coordination of the Te atom is strongly asymmetric: For the atom shown in Fig. 1(a), only the “c” contacts are in the (slightly) negative  $y$  direction.

The coordination of this new high-pressure structure is thus quite complex—surprisingly so for a phase well above 10 GPa. But the range of interatomic distances and the fact that the close coordination is fivefold accounts for the problems encountered in fitting the recent EXAFS data. Also, preliminary results from studies of CdTe and HgTe suggest that they, too, exhibit the same structure; it is not a peculiarity of ZnTe. What emerges is thus the *similarity* of ZnTe to the other tellurides, rather than the quite different structural behavior it has previously been believed to show. All three tellurides are now known to transform from zinc blende to a cinnabar (or cinnabarlike) phase and appear to share the new *Cmcm* structure at higher pressures. ZnTe differs only in having no intermediate NaCl phase.

Finally, the unusual coordination and relative complexity of the *Cmcm* structure probably account for its solution having proved difficult with previously available techniques. The results presented here all depend on the high sensitivity and 2D nature of image-plate data, which make it possible to use anomalous dispersion, detect very weak reflections, and survey preferred orientation. All these were necessary in reaching the proposed solution.

We thank A. Polian and J.P. Itié of Université Paris VI for kindly supplying the sample crystal. We gratefully acknowledge the assistance of our colleague J. S. Loveday in various aspects of the experimental work and would like to thank A. A. Neild and G. Bushnell-Wye of the Daresbury Laboratory for their help in preparing the beam-line equipment. This work is supported by a grant from the Engineering and Physical Sciences Research Council and by facilities made available by Daresbury Laboratory. Valued assistance with the maintenance and development of pressure cells has been given by D.M. Adams of Diacell Products.

---

[1] P. L. Smith and J. E. Martin, Phys. Lett. **19**, 541 (1965).

- [2] S. Ves, U. Schwarz, N.E. Christensen, K. Syassen, and M. Cardona, Phys. Rev. B **42**, 9113 (1990).
- [3] M.I. McMahon, R.J. Nelmes, N.G. Wright, and D.R. Allan, Phys. Rev. B **48**, 16 246 (1993).
- [4] A. Werner, H.D. Hochheimer, K. Strössner, and A. Jayaraman, Phys. Rev. B **28**, 3330 (1983).
- [5] G. A. Samara and H. G. Drickamer, J. Phys. Chem. Solids **23**, 457 (1962).
- [6] A. Ohtani, M. Motobayashi, and A. Onodera, Phys. Lett. **75A**, 435 (1980).
- [7] K. Strössner, S. Ves, W. Honle, W. Gebhardt, and M. Cardona, in *Proceedings of the 18th International Conference on the Physics of Semiconductors, Stockholm, 1986*, edited by O. Engstrom (World Scientific, Singapore, 1987), p. 1717.
- [8] A. San-Miguel, A. Polian, J.P. Itié, A. Marbeuf, and R. Triboulet, High Pressure Research **10**, 412 (1992); A. San-Miguel, A. Polian, M. Gauthier, and J.P. Itié, Phys. Rev. B **48**, 8683 (1993).
- [9] M.I. McMahon, R.J. Nelmes, N.G. Wright, and D.R. Allan, in Proceedings of the Joint AIRAPT/APS Topical Conference on High Pressure Science and Technology, Colorado Springs, 1993, edited by S. Schmidt (American Institute of Physics, New York, to be published).
- [10] R.J. Nelmes, P.D. Hatton, M.I. McMahon, R.O. Piltz, J. Crain, R.J. Cernik, and G. Bushnell-Wye, Rev. Sci. Instrum. **63**, 1039 (1992).
- [11] R.O. Piltz, M.I. McMahon, J. Crain, P.D. Hatton, R.J. Nelmes, R.J. Cernik, and G. Bushnell-Wye, Rev. Sci. Instrum. **63**, 700 (1992).
- [12] R.J. Nelmes and M.I. McMahon, “Advances in X-Ray Analysis” Vol. 43 (to be published).
- [13] D.M. Adams, Diacell Products, 54 Ash Tree Road, Leicester, United Kingdom.
- [14] G.F. Piermarini, S. Block, J.D. Barnett, and R.A. Forman, J. Appl. Phys. **46**, 2774 (1975).
- [15] H.M. Rietveld, J. Appl. Crystallogr. **2**, 65 (1969).
- [16] A. N. Fitch and A. D. Murray, report, 1990 (unpublished).
- [17] M.I. McMahon, R.J. Nelmes, N.G. Wright, and D.R. Allan (to be published).
- [18] Anomalous dispersion effects alter the relative scattering power of Cd and Te between the two wavelengths used. That gives rise to changes in the relative intensities of reflections, particularly weak reflections in which Cd and Te scatter in antiphase and thus almost cancel out, provided the structure is site ordered.